Reduced-Order Compensator Design for a Flexible Structure

Ph. C. Opdenacker,* E. A. Jonckheere,† M. G. Safonov,‡ J. C. Juang§
University of Southern California, Los Angeles, California
and
M. S. Lukich¶
TRW, Redondo Beach, California

A low-order controller is designed for an experimental truss structure. The objective is to achieve good disturbance attenuation, while at the same time preserving good stability margin and other robustness properties. The method used is linear quadratic Gaussian (LQG) with frequency dependent weights and colored noises for shaping singular-value Bode plots. Controller reduction is accomplished through the open-loop balancing scheme applied to the full-order compensator. A typical design result shows that it is possible to obtain a very low-order design that meets the preceding specification.

Introduction and Problem Statement

THE experimental truss structure under study is shown in Fig. 1 and is described in detail in Major and Simonian.[20] This structure was designed and built to be a test bed for the preliminary study of large flexible space structure control for optical missions. The top and bottom plates are assumed to be rigid bodies and represent mirrors whose relative position (y_o) must be controlled very accurately. The two plates are interconnected by a flexible rod assembly. It consists of four load-bearing corner posts and four diagonal members that are not loaded but contain four force-generating actuators (u) for active control. The structure is excited by two momentum exchange devices (d_m) mounted on the top platform. In this experiment, we have adopted the point of view that the most accurate active control would be achieved if precisely those variables that are to be controlled (y_o) could be sensed. Therefore, four optical detectors measure the relative displacement (y_m) of the plates. Observe that the actuators and the sensors are *not* colocated. The open-loop dynamics of the structure is described by

$$y_o = \underbrace{C(sI - A)^{-1}B_m}_{G_m(s)} d_m + \underbrace{C(sI - A)^{-1}B_o}_{G_o(s)} u$$

$$y_m = y_o + n$$

In the description, d_m is the disturbance, u the control actuator input, and y_o the output-to-be-controlled. The sensor output y_m is, up to a measurement noise n, the output-to-be-controlled y_o. In this experiment, the four sensor outputs are not linearly independent; more precisely, the rows of C are linearly dependent. In this design, to avoid some technical difficulties, we will discard one row of the matrix C, and from now on we will assume that the matrix C has three linearly independent rows and that the vector y_o is three-dimensional. In summary,

$$dim(u) = 4,$$

$$dim(d_m) = 2$$

$$dim(y_o) = dim(y_m) = dim(n) = 3$$

The matrix A is 40×40, accounting for 20 vibration modes. There are no rigid body modes. The modal data (A, B_m, B_o, C) have been computed through a finite element analysis of the structure. These are provided in Table A1. The first three modes represent the foremost part of the disturbance transmission; they occur at frequencies of 4.84, 5.14,

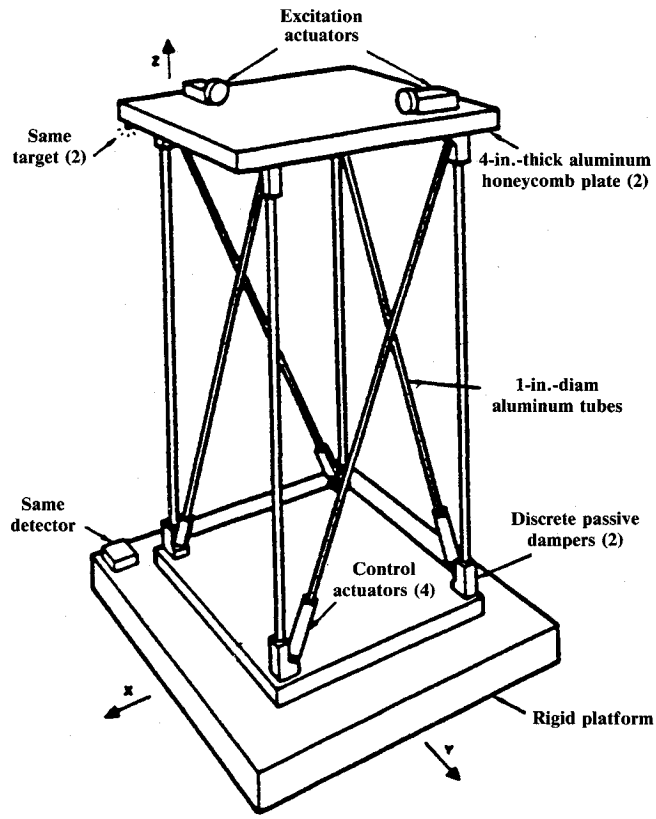

Fig. 1 Truss experiment configuration.

Received May 5, 1986; revision received June 27, 1988.

*Research Assistant. Department of Electrical Engineering-Systems.
†Associate Professor. Department of Electrical Engineering-Systems.
‡Professor. Department of Electrical Engineering-Systems.
§Research Associate. Department of Electrical Engineering-Systems.
¶Member. Technical Staff.

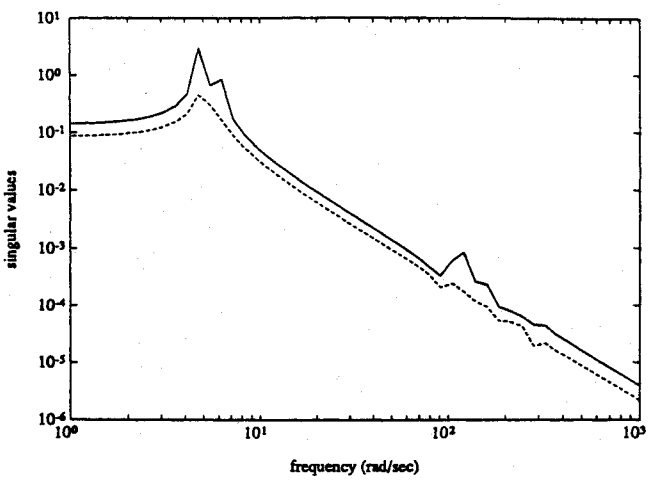

Fig. 2 Open-loop disturbance response.

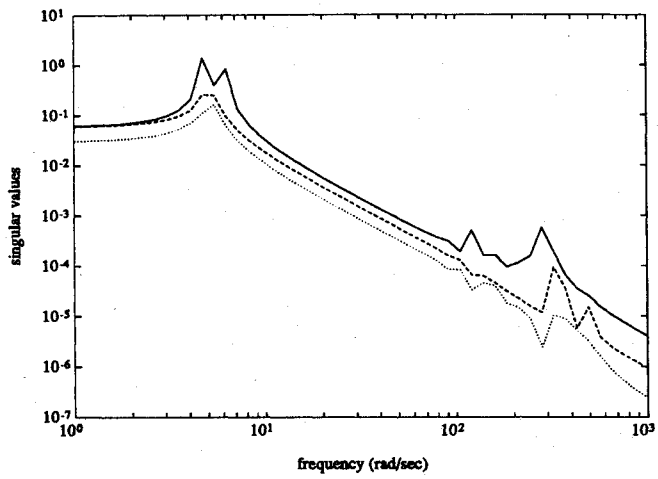

Fig. 3 Open-loop transfer function.

and 6.06 rad/s, respectively. The open-loop singular value plot of the disturbance response is shown in Fig. 2; the singular value plot of the plant transfer function (from the control actuators to the sensor outputs) is shown in Fig. 3. The first three modes induce a large resonance peak in the plant transfer matrix from the control actuators to the sensor outputs, as well as in the transfer matrix from the disturbances to the outputs. There is no need to convince the reader that these open-loop responses are highly unsatisfactory. The need for damping the resonance peak around 5 rad/s is obvious.

The purpose of this experiment is to design a *low-order* feedback controller $K(s)$, such that the closed-loop transmission from the disturbance d_m to the relative displacement y_o of the plates is "small" (in a sense to be made precise later). The feedback must incorporate enough stability robustness, for the structure modal data (A, B_m, B_o, C) could be off as much as 100% or more in the higher frequency range beyond about 100 rad/s. Another source of uncertainty is the digital computer implementation of the controller, the delay of which requires a certain amount of phase margin. (Of course, this source of uncertainty could have been eliminated if we had elected to do a discrete-time LQG design.)

The design methodology is frequency-weighted linear quadratic Gaussian (LQG)[11] applied to the *full-order* system (including the 20 vibration modes and the shaping filters) followed by balanced reduction[1] of the full-order LQG compensator. The use of the full-order plant model instead of reduced-order plant model in the controller design stage is aimed at taking into consideration as many potentially important modes as possible. An H^∞ controller has also been designed for the same structure,[21] which, because of computational considerations, was based on the *reduced-order* plant model.

Frequency-Weighted LQG Design Approach

The LQG/Wiener-Hopf design method is well known to naturally take care of rms disturbance attenuation; stability margin measures are also included in the criterion being optimized. LQG design with white noises and constant weights did not perform in a satisfactory way. It was, therefore, decided to make use of colored noises and frequency-dependent weights on the plant output, following the procedure suggested by Safonov et al.[11] for selecting the frequency-dependent weights and noises. This procedure involves manipulation of singular-value Bode plots via iterative adjustment of frequency-dependent cost and noise matrix parameters.

The problem to be solved is then a usual LQG design problem for an augmented state-space description of the plant together with the noise dynamics and the output weighting. Namely, we want to minimize the following criterion:

$$J = E(q_o z^T z + r_o u^T u) \tag{1}$$

subject to

$$\dot{x} = Ax + B_o u + B_o d_o + B_m d_m \tag{2a}$$

$$\dot{z} = -\beta z + \beta y_o \tag{2b}$$

$$\dot{d}_m = -\alpha d_m + \alpha v_1 \tag{2c}$$

$$\dot{\xi} = -\gamma \xi + (\delta - \gamma) v_2 \tag{2d}$$

$$y_o = Cx \tag{2e}$$

$$y_m = Cx + n \tag{2f}$$

$$n = \xi + v_2 \tag{2g}$$

where the following notation is used:

x: state of the original plant [$dim(x) = 40$]
u: control actuator input [$dim(u) = 4$]
y_o: plant output, i.e., relative position of the plates, to be controlled
y_m: sensor output [$dim(y_o) = dim(y_m) = 3$]
z: frequency weighted plant output [$dim(z) = 3$]
d_o, v_1, v_2: Gaussian white noises with intensities q_s, q_m, $r_m(\gamma/\delta)^2$, respectively
d_m: colored disturbance acting on the structure [$dim(d_m) = 2$]
n: colored measurement noise
ξ: state of the filter used to generate the measurement noise

The design scalar parameters, all of which are positive, are α, β, γ, δ, r_m, q_m, q_s, r_o, and q_o.

It is easily seen that z and d_m are outputs of first-order low-pass filters and, provided that one chooses $\delta < \gamma$, then n is the output of a first-order high-pass filter. The complete feedback system is illustrated in Fig. 4. The rationale behind this choice is as follows:

1) The disturbance d_m generated by the momentum exchange device is assumed to be a bandlimited noise with cutoff frequency at 15 Hz. The low-pass filter $\alpha/(s+\alpha)$ reflects the nature of this disturbance. The parameter α, on the one hand, is used to emulate the physical situation; on the other hand, it is a design parameter that the designer can adjust to account

for global system performance without distorting its fundamental physical significance.

2) A fictitious noise, d_o, is used to enhance stability margin at the input. Indeed, the intensity of this fictitious noise can be physically interpreted as the extent of uncertainty on the actuator. In the design procedure, the designer is in need of the flexibility offered by this parameter for stability margin enhancement. The noise is chosen white because its wide band covers the entire frequency spectrum over which uncertainties can occur.

3) A usual rule of thumb used for finite element models of flexible structures says that only about the very first natural eigenfrequencies and mode shapes can be accurately predicted. To counteract this, the measurement noise n is used to improve the stability margin and the robustness properties of the closed-loop system at high frequencies, where model uncertainty becomes important. The filter $(s+\delta)/(s+\gamma)$ that generates n is high pass, provided $\delta < \gamma$.

4) In the quadratic criterion, we penalize z, a frequency weighted version of y_o. The reason for penalizing z rather than y_o is that the low-frequency component of y_o picks up most of the actual mechanical motion.

The introduction of the preceding *artificial* signals and filters does have its physical interpretation (see also Ref. 18). Mathematically, the design parameters resemble weighting functions used to tune the optimization procedure. This weighting strategy is made clearer by rewriting the cost in the frequency domain as follows:

$$J = \frac{1}{2}\int_{-\infty}^{\infty} Tr[T(jw)T^*(jw)]dw \tag{3}$$

where $T(jw)$ is the closed-loop transfer function from input

$$\begin{bmatrix} q_s^{-1/2}d_o \\ q_m^{-1/2}v_1 \\ r_m^{-1/2}\left(\frac{\delta}{\gamma}\right)v_2 \end{bmatrix}$$

to output

$$\begin{bmatrix} q_o^{1/2}z \\ r_o^{1/2}u \end{bmatrix}$$

$$T(s) = \begin{bmatrix} \frac{q_o^{1/2}\beta}{s+\beta}I & 0 \\ 0 & r_o^{1/2}I \end{bmatrix} \begin{bmatrix} S(s) & S(s) & G_oW(s) \\ W(s) & W(s) & W(s) \end{bmatrix}$$

$$\times \begin{bmatrix} q_s^{1/2}G_o(s) & 0 & 0 \\ 0 & \frac{q_m^{1/2}\alpha}{s+\alpha}G_m(s) & 0 \\ 0 & 0 & r_m^{1/2}\frac{\gamma(s+\delta)}{\delta(s+\gamma)} \end{bmatrix} \tag{4}$$

where

$$S(s) := [I + G_o(s)K(s)]^{-1} \tag{5a}$$

$$W(s) := K(s)[I + G_o(s)K(s)]^{-1} \tag{5b}$$

and

$$G_o(s) := C(sI - A)^{-1}B_o \tag{6a}$$

$$G_m(s) := C(sI - A)^{-1}B_m \tag{6b}$$

G_i and G_i^* are short for $G_i(jw)$ and $G_i^T(-jw)$, respectively, $i = o, m$.

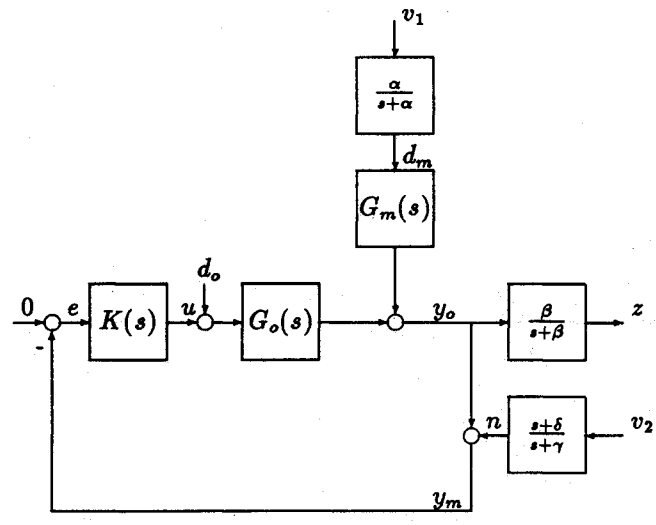

Fig. 4 Control system configuration with fictitious noises and weightings.

The effect of each of the design parameters as frequency varies can be more easily understood from Eq. (4) than in the time domain (see Ref. 7). The main goal of the design being to obtain a large attenuation of the transmission $S(s)G_m(s)$ from the disturbance d_m to the output y_o, it is clear that we should try to make the size of $S(s)$ as small as possible. Equivalently, we have to make the products q_oq_s and q_oq_m large. This way, the sensitivity $S(s)$ will be very small whenever G_o and G_m are large; that is, exactly at the resonant peak around $w = 5,...,6$ rad/s. The goal of making $S(s)$ small must be traded off against the necessity of maintaining a sufficient stability margin to tolerate plant modeling uncertainty. As is well known, the stability margin at each frequency w is inversely proportional to the singular-values of $W(jw)$. The size of the smallest *additive* perturbation $\delta G(jw)$ for which the closed-loop is unstable when the plant G_o is perturbed to $G_o(jw) + \delta G(jw)$ is precisely[11,13]

$$\sigma_{\max}[\delta G(jw)] = \frac{1}{\sigma_{\max}[W(jw)]} \tag{7}$$

Similarly, it is known[11,13] that the size of the smallest *multiplicative* perturbation $\Delta(jw)$ that causes instability when the plant is perturbed to $[I + \Delta(jw)]G_o(jw)$ is

$$\sigma_{\max}[\Delta(jw)] = \frac{1}{\sigma_{\max}[G_o(jw)W(jw)]} \equiv \frac{1}{\sigma_{\max}[I - S(jw)]} \tag{8}$$

In our problem, the plant is known reasonably accurately up to only about 100 rad/s; at higher frequencies, modeling uncertainty approaching 100% or more arises because of the many imprecisely known high-frequency modes of the plant. Accordingly, if we assume that the uncertainty $\Delta(jw)$ grows with a rate not exceeding 20 dB/decade beyond 100 rad/s, we require our design to satisfy the stability margin specification

$$\sigma_{\max}[I - S(jw)] \leq -20\log_{10}\left(\frac{w}{100}\right), \quad \forall w \geq 100 \text{ rad/s} \tag{9}$$

Sensitivity and robustness properties of the linear quadratic regulator or the Kalman-Bucy filter are well known.[15] However, when the two are combined to design a LQG compensator, no a priori robustness measure can be assessed.[16] Therefore, while tuning the parameters to ensure low sensitivity, we checked stability and gain and phase margins repeatedly. The reader should keep in mind that "optimality" does not guarantee good design properties, like robustness and stability margin. To apply the frequency-weighted LQG cost

function design approach of Ref. 11 to the current design problem, one begins by examining how and over what frequency ranges the design parameters (q_o, r_o, β, q_s, q_m, α, r_m, γ, δ) penalize sensitivity $S(jw)$ and stability margin $W(jw)$ at each frequency. First, note that at lower frequencies, where $q_s^{1/2}G_o(jw)$ and $[q_m^{1/2}\alpha/(s+\alpha)]G_m(s)$ are big compared to $r_m^{1/2}[\gamma(s+\delta)/\delta(s+\gamma)]$, one has that the term $T(s)$ in the cost of Eq. (3) becomes approximately

$$T(s) \simeq \begin{bmatrix} \frac{q_o^{1/2}\beta}{s+\beta} I & 0 \\ 0 & r_0^{1/2} I \end{bmatrix} \begin{bmatrix} S(s) & S(s) \\ W(s) & W(s) \end{bmatrix} \times \begin{bmatrix} q_s^{1/2}G_o(s) & 0 \\ 0 & \frac{q_m^{1/2}\alpha}{s+\alpha} G_m(s) \end{bmatrix} \tag{10}$$

whereas at higher frequencies one has approximately

$$T(jw) \simeq \begin{bmatrix} \frac{q_o^{1/2}\beta}{s+\beta} I & 0 \\ 0 & r_0^{1/2} I \end{bmatrix} \begin{bmatrix} G_o(s)W(s) \\ W(s) \end{bmatrix} r_m^{1/2} \frac{\gamma(s+\delta)}{\delta(s+\gamma)} \tag{11}$$

Thus, at the higher frequencies, the LQG optimal controller focuses entirely on making $W(s)$ small (and hence on making the stability margin big). However, in the lower frequency range and up to the frequency where $[r_m^{1/2}\gamma(s+\delta)/\delta(s+\gamma)]$ dominates the right term in Eq. (4), there is the possibility of trading off $S(s)$ vs $W(s)$ by increasing $q_o^{1/2}\beta/(s+\beta)$ or $r_o^{1/2}$, respectively.

Another important consideration, dictated by the methodology of reducing the compensator using the balancing technique, is stability of the LQG compensator, which is not always guaranteed. In addition to this stability requirement, the LQG compensator should also exhibit a big spread of Hankel singular values, so that its reduction entails only a small frequency response error that, in turn, guarantees preservation of most of the robustness and sensitivity properties of the loop.

Using the foregoing considerations as a guide for adjusting the design parameters and keeping in mind that the design objective is to make $\sigma_i[S(jw)G_m(jw)]$ as small as possible up to about $w = 30$ rad/s, subject to the stability margin constraint of Eq. (9) at frequencies $w \geq 100$ rad/s, we arrived at a choice for the design parameters after several LQG design iterations. The following parameters yielded a reasonable tradeoff between disturbance rejection, stability margins, and ability to reduce the compensator:

$$q_o = 2 \times 10^7$$

$$r_o = 1$$

$$q_m = 5 \times 10^6$$

$$q_s = 5 \times 10^6$$

$$r_m = 40$$

$$\alpha = 100 \text{ rad/s}$$

$$\beta = 100 \text{ rad/s}$$

$$\gamma = 120 \text{ rad/s}$$

$$\delta = 0.1\gamma$$

Controller Design Details

Stacking together Eq. (2) yields the augmented equations

$$\begin{bmatrix} \dot{x} \\ \dot{z} \\ \dot{d}_m \\ \dot{\xi} \end{bmatrix} = A_a \begin{bmatrix} x \\ z \\ d_m \\ \xi \end{bmatrix} + B_{oa}u + B_{ma} \begin{bmatrix} v_1 \\ d_o \\ v_2 \end{bmatrix} \tag{12a}$$

$$z = \underbrace{[0 \quad I \quad 0 \quad 0]}_{C_{oa}} \begin{bmatrix} x \\ z \\ d_m \\ \xi \end{bmatrix} \tag{12b}$$

$$y_m = \underbrace{[C \quad 0 \quad 0 \quad I]}_{C_{ma}} \begin{bmatrix} x \\ z \\ d_m \\ \xi \end{bmatrix} + v_{2_1} \tag{12c}$$

where

$$A_a = \begin{bmatrix} A & 0 & B_m & 0 \\ \beta C & -\beta I & 0 & 0 \\ 0 & 0 & -\alpha I & 0 \\ 0 & 0 & 0 & -\gamma I \end{bmatrix} \tag{13a}$$

$$B_{oa} = \begin{bmatrix} B_o \\ 0 \\ 0 \\ 0 \end{bmatrix} \tag{13b}$$

$$B_{ma} = \begin{bmatrix} 0 & B_o & 0 \\ 0 & 0 & 0 \\ \alpha I & 0 & 0 \\ 0 & 0 & (\delta - \gamma)I \end{bmatrix} \tag{13c}$$

Control Equation

$$A_a^T P_a + P_a A_a + q_o C_{oa}^T C_{oa} - (1/r_o) P_a B_{oa} B_{oa}^T P_a = 0 \tag{14}$$

For existence and uniqueness of a positive semidefinite, stabilizing solution P_a of Eq. (14), we need the pair (A_a, B_{oa}) to be stabilizable and the pair (A_a, C_{oa}) to be detectable. Clearly, the state ξ is neither controllable from u nor observable from z, although it is stabilizable and detectable. Hence, the fourth row and column blocks of P_a will be zero.

Filtering Equation

Because of the presence of v_2 in Eq. (12a), the plant noise and the measurement noise are correlated; the filtering Riccati equation must be altered to account for this (see Ref. 19).

Let

$$V_2\delta(t) := E(v_2 v_2^T) = r_m \left(\frac{\gamma}{\delta}\right)^2 I\delta(t) \tag{15a}$$

$$V_1\delta(t) := E\left(\begin{bmatrix} v_1 \\ d_o \\ v_2 \end{bmatrix} [v_1^T \quad d_o^T \quad v_2^T] \right) = E\left(\begin{bmatrix} v_1 v_1^T & 0 & 0 \\ 0 & d_o d_o^T & 0 \\ 0 & 0 & v_2 v_2^T \end{bmatrix} \right) = \begin{bmatrix} q_m I & 0 & 0 \\ 0 & q_s I & 0 \\ 0 & 0 & r_m \left(\frac{\gamma}{\delta}\right)^2 I \end{bmatrix} \delta(t) \tag{15b}$$

$$V_{12}\delta(t) := E\left(\begin{bmatrix} v_1 \\ d_o \\ v_2 \end{bmatrix} v_2^T\right) = \begin{bmatrix} 0 \\ 0 \\ V_2 \end{bmatrix}\delta(t) \qquad (15c)$$

The modified filtering equation is then given by

$$A_f S_a + S_a A_f^T - S_a C_{ma}^T V_2^{-1} C_{ma} S_a + B_{ma} W_f B_{ma}^T = 0 \qquad (16)$$

where $A_f := A_a - B_{ma}V_{12}V_2^{-1}C_{ma}$ and $W_f := V_1 - V_{12}V_2^{-1}V_{12}^T$.

The Kalman filter gain becomes

$$K_f = (S_a C_{ma}^T + B_{ma}V_{12})V_2^{-1} \qquad (17)$$

It can be shown (see Ref. 18) that the triple $(A_f, B_{ma}W_f^{1/2}, C_{ma})$ is minimal; therefore, the stabilizing solution S_a exists, is unique, and is positive definite.

Controller Reduction

The high order of the system requires a reliable numerical method, such as that described in Laub.[14] Since the augmented state vector has dimension 48, the compensator itself involves 48 states, which makes its use in real time highly impractical. Hence, we have to reduce the order of the compensator, at the same time preserving 1) stability of the closed-loop system, 2) good disturbance rejection, and 3) stability margin. As we have seen before, a few methods for doing this are available in the literature. A most interesting result was obtained independently by Enns[8] and Glover.[2] They showed that the error made in approximating a stable system by the open-loop balancing method of Moore[1] can be bounded in the infinity norm, as follows.

Let $K(s)$ and $K_r(s)$ denote the full and the reduced systems of order r, respectively, and σ_i the ith Hankel Singular Value of $K(s)$ (the σ_i's are in decreasing order). Then we have

$$\|K(s) - K_r(s)\|_\infty \le 2 \sum_{i=r+1}^{n} \sigma_i \qquad (18)$$

This result shows that the Nyquist diagrams of the reduced and full compensators remain close together. Hence, if the order of the reduced compensator is properly chosen, i.e., if $\Sigma_{i=r+1}^{n}\sigma_i$ is small enough, the reduction procedure should not affect the closed-loop properties of the system too much. Recently, a similar result, but with tighter error bounds, was obtained by Opdenacker and Jonckheere for the new balancing method described in Ref. 3.

The realization of the full-order controller is provided in Tables B1a and B1b. It can be checked that our compensator is asymptotically stable and, therefore, we are allowed to use the open-loop balancing model reduction method to come up with a controller of smaller size. The Hankel singular values of the full-order controller $K(s)$ are provided in Fig. 5. A controller of *order 10* (down from 48) was obtained as a tradeoff between retaining very closely the properties of the full-order design and having sufficiently low order for implementation. (It is worth mentioning that a (stabilizing) controller of *order 6* can be obtained using the new balancing

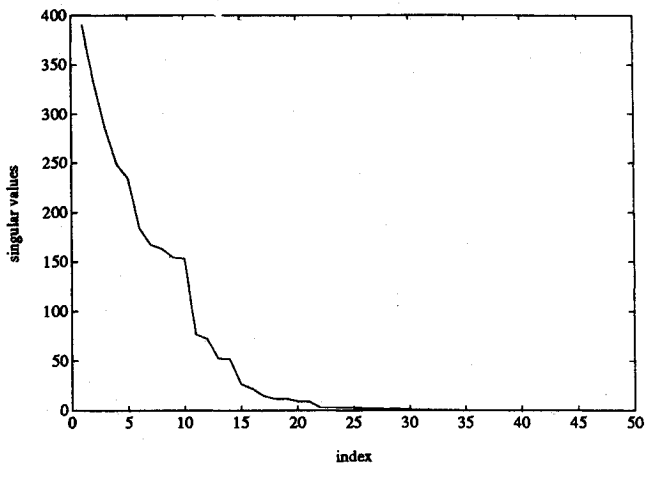

Fig. 5 Hankel singular values of the full-order controller.

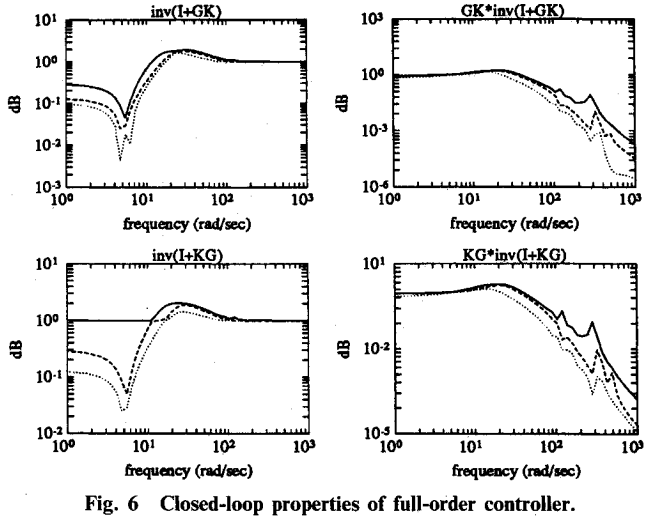

Fig. 6 Closed-loop properties of full-order controller.

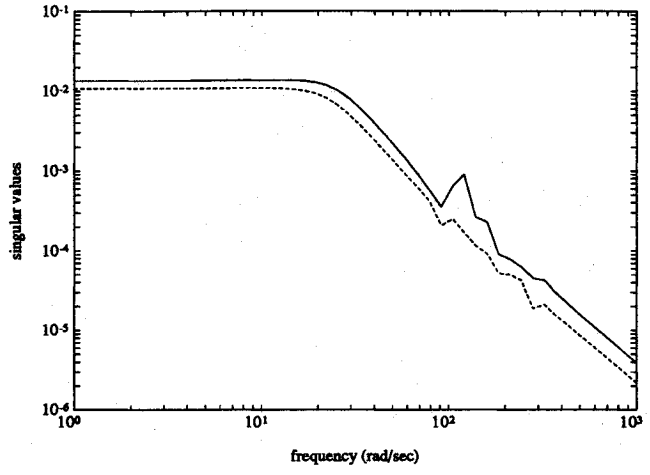

Fig. 7 Disturbance response using full-order controller.

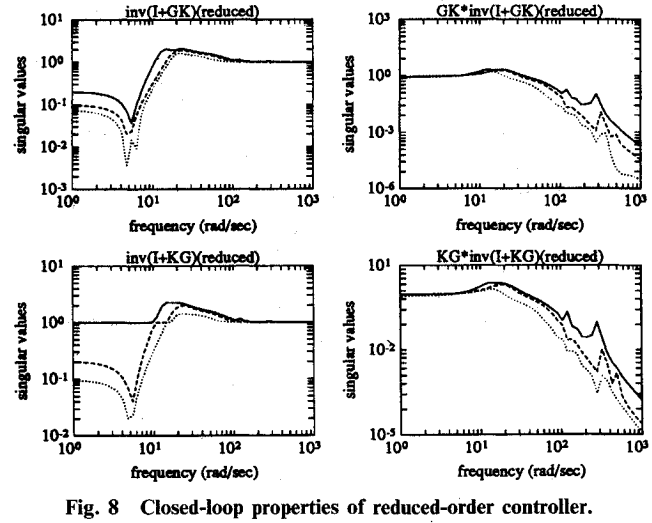

Fig. 8 Closed-loop properties of reduced-order controller.

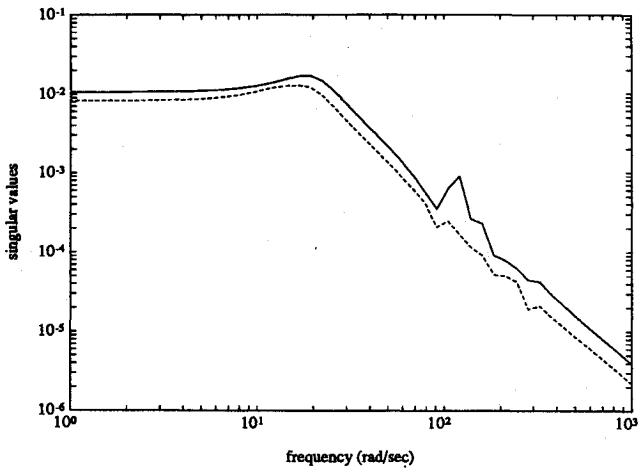

Fig. 9 Disturbance response using reduced-order controller.

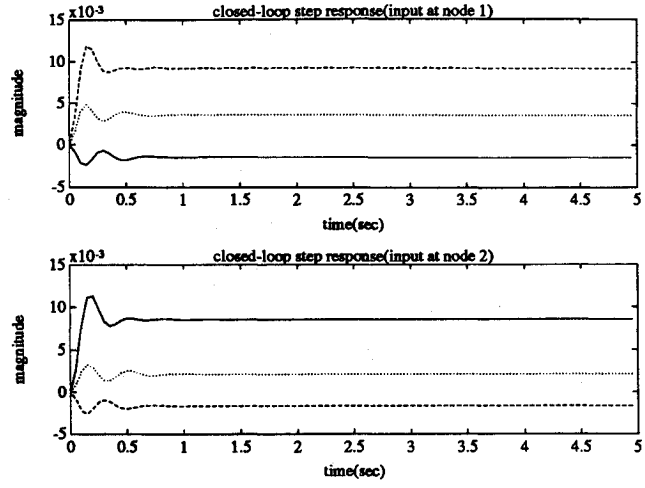

Fig. 10 Closed-loop step response.

technique of Opdenacker and Jonckheere.[3]) The reduced-order controller is tabulated in Table C1. The simulation results of these two controllers can be checked by comparing Figs. 6 and 7 with Figs. 8 and 9. As can be seen, the full-order and reduced-order compensator plots of the stability margins $(I + KG_o)^{-1}KG_o$ and $(I + G_oK)^{-1}G_oK$ are roughly indistinguishable. Regarding disturbance transmission, the only noticeable effect of the reduction of the controller is a (surprising) 2 dB drop of noise transmission at frequency $w < 30$ rad/s, followed by a small hump in the singular value plot occurring at $w \simeq 30$ rad/s, as can be seen from Figs. 7 and 9.

The procedure for model reduction goes as follows:

1) Compute the state-space description of the compensator as

$$\dot{\eta} = F\eta + Gy_m$$

$$u = -H\eta$$

where

$$F = A_a - \frac{1}{r_o} B_{oa}B_{oa}^T P_a - K_f C_{ma}$$

$$G = K_f$$

$$H = \frac{1}{r_o} B_{oa}^T P_a$$

Check for stability of F. In the present case, F is stable.

2) Compute a new balanced representation of (F, G, H), say $(\hat{F}, \hat{G}, \hat{H})$, which is open-loop balanced (Ref. 1).

3) Keep the states of compensators with the largest characteristic values, and check for stability of the closed-loop system made up with the full plant and the reduced compensator.

4) Check SVD plots to make sure that the reduction procedure does not destroy sensitivity and robustness properties of the full design.

Implementation

For real-time implementation, the controller has to be discretized. This was done assuming the presence of a zero-order hold and a sampling period $T_s = 5$ ms. The algorithm used is described in Kallstrom.[9] The discretized compensator was implemented with the block diagonal form of the $10 \times$ *10 matrix F_r of the compensator. This is indeed compatible with the number of operations (per second) the digital controller could sustain. Because of the short sampling period, the discretization did not affect the performance over the bandwidth of interest ($2\pi/T_s > 30$ rad/s). Because the gain cross-over occurs at $w \simeq 30$ rad/s, the phase shift induced by discretization, $\angle e^{-j30*T_s} \simeq -3$ deg, is negligible with respect to the 30-deg phase margin.

Performance Analysis of the Design

Typical time responses with the reduced controller of order 10 are shown in Figs. 10 and 11 for the same disturbances as in the open-loop situation (Figs. 12 and 13). To quantify the improvement, we choose a sine wave disturbance at $w = 5$ rad/s (resonant frequency); if we then define the attenuation to be the ratio of the *peak-to-peak* open-loop output amplitude and the *peak-to-peak* closed-loop output amplitude, we deduce (from Figs. 11 and 13) that the improvement is about 100. This is a somewhat optimistic measure because the system is excited at the *resonant frequency*, yielding an open-loop output wave containing a secular term $te^{-0.03t} \sin 5t$, (see Fig. 13) and hence a large peak-to-peak amplitude.

For another time domain measure of improvement, see Ref. 22. The improvement is measured rather as the ratio of the open-loop and closed-loop output noise amplitudes under random bandlimited excitation.

Aside from the closed-loop time responses mentioned previously, singular value plots were computed. Figures 8 and 9 show the improvement in noise transmission, as well as sensitivity and loop functions, and measures of robustness. It can be seen that the system can tolerate variations of approximately 50% of the loop function, and it also indicates a gain margin of approximately 15 dB and a phase margin of 30 deg.

There are several criteria for measuring the improvement in disturbance attenuation of the controller. One of them is the rms criterion. Let T_{OL} and T_{CL} denote the open-loop and closed-loop transmissions from disturbance d_m to output y_o, respectively. Then, the rms attenuation ratio AR can be defined as

$$AR = \left[\frac{\int_0^{w_o} \sum_{i=1}^{2} \sigma_i^2(T_{OL})dw}{\int_0^{w_o} \sum_{i=1}^{2} \sigma_i^2(T_{CL})dw} \right]^{1/2} \tag{19}$$

where w_o denotes the frequency band of interest. Here $w_o \simeq 30$ rad/s, and for the reduced controller, we get $AR \simeq 30$ dB, which, interestingly enough, is superior to that of the full-order design by about 2 dB. For $w_o = 90$ rad/s, we still get $AR \simeq 29$ dB. For $w_o \simeq 5$ rad/s, which is the resonance

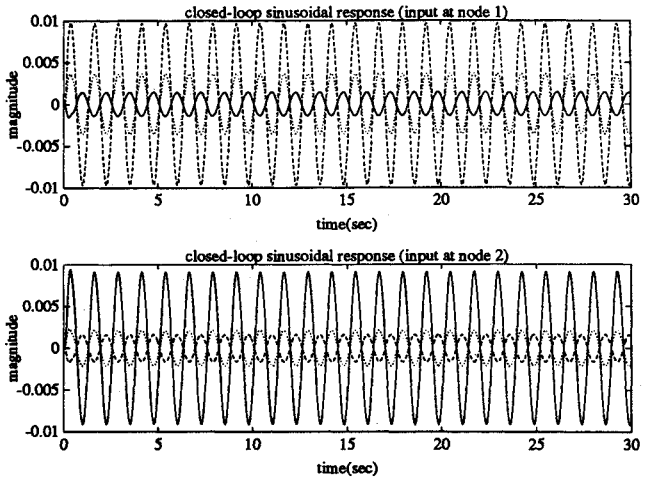

Fig. 11 Closed-loop sinusoidal response.

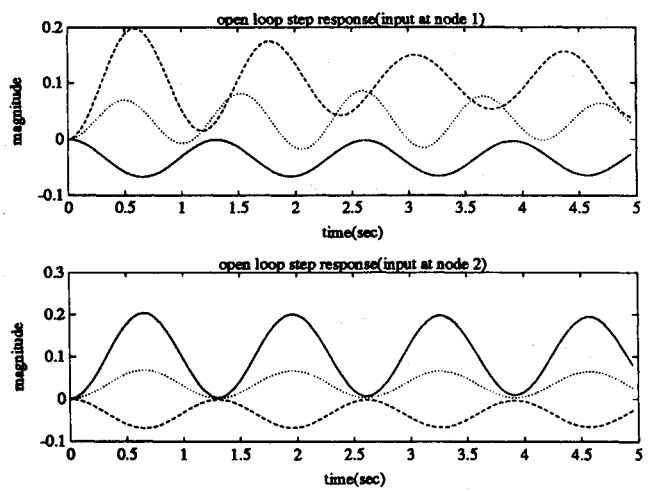

Fig. 12 Open-loop step response.

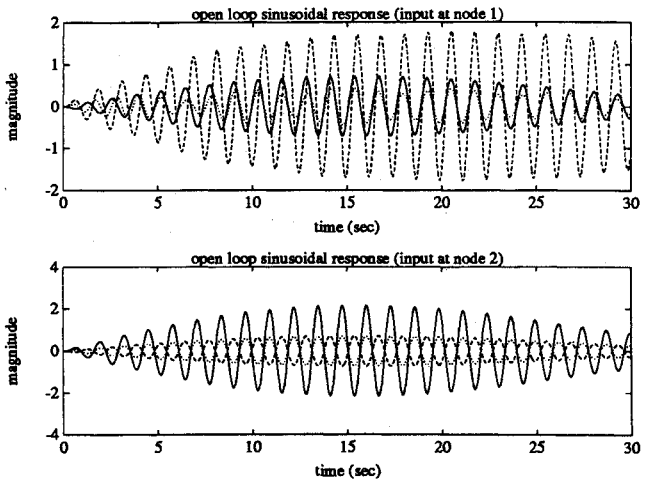

Fig. 13 Open-loop sinusoidal response.

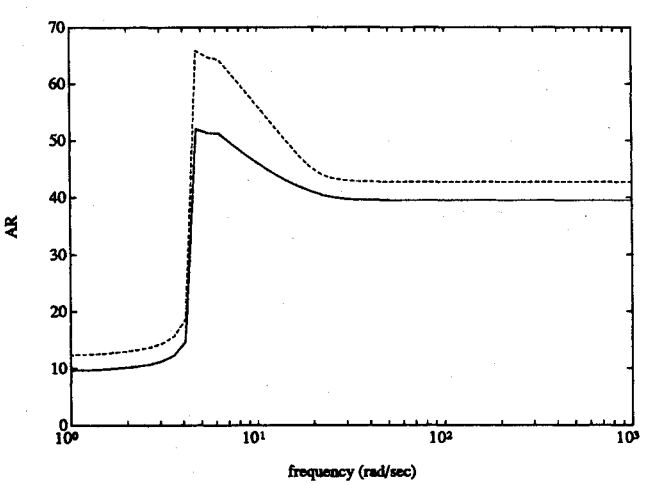

Fig. 14 The attenuation ratios (AR's) of the full-order controller (solid) and the reduced-order controller (dotted).

frequency, $AR \simeq 32$ dB (for the reduced-order controller); the controller has indeed put an effort in attenuating the vibration. These attenuation ratio results are clearly shown in Fig. 14. Besides the method used in Eq. (19), there are other ways of quantifying the attenuation ratio in the frequency domain. In Ref. 22, the attenuation ratio is rather related to the loop characteristic gains at low frequency.

Laboratory Test of Design

The designed compensator was digitally implemented and tested in a real laboratory experiment that was conducted in March 1985. The colored noise sequence was stored in the control program's memory and passed through D/A converters to the disturbance actuator's amplifiers. The design proved successful on the first try. The compensator was still stabilizing; however, the attenuation ratio was not as good as that predicted by the simulation studies (see Ref. 22 for the lab test report).

Actually, it appears that the compensator design procedure described in this paper is too cautious, in the sense that the laboratory experiment has indicated that the controller has too much stability margin, despite the inherent uncertainties that plague such complex systems as flexible structures. It seems at this point that sacrificing some stability margin to improve the attenuation ratio would lead to a better trade-off.

Conclusion

The frequency-weighted LQG feedback synthesis procedure in conjunction with balancing model reduction techniques has been successfully applied to the design of a robust multiloop controller for an experimental flexible structure. The design required iterations on the weights. Simulation studies predicted good robustness and $AR \simeq 30$ dB of disturbance attenuation over the closed-loop bandwidth 0 to 30 rad/s. The resulting controller worked satisfactorily on the physical system on the first try without further modification.

Appendix A

The 4×4 plant transfer function matrix $G_o(s)$ and the 4×2 disturbance model $G_m(s)$ can be represented as

$$G_o(s) = \sum_{i=1}^{20} \frac{c_i b_i}{s^2 + \zeta_i s + w_i^2}$$

and

$$G_m(s) = \sum_{i=1}^{20} \frac{c_i b_{mi}}{s^2 + \zeta_i s + w_i^2}$$

Table A1 The plant transfer function and the disturbance model

1	2.3151D + 01	4.8116D − 02	2.2402D − 01	6.6712D − 01	2.2320D − 01	−2.1989D − 01
	5.1010D − 01	−1.5438D + 00	−1.5438D + 00	5.1717D − 01	−5.0950D − 01	−5.1718D − 01
2	2.6442D + 01	5.1422D − 02	−5.8205D − 01	5.3961D − 04	5.8205D − 01	−5.3937D − 04
	−1.3290D + 00	9.4707D − 06	8.8020D − 06	−1.3474D + 00	8.4377D − 06	−1.3474D + 00
3	3.6718D + 01	6.0595D − 02	3.9477D − 01	−2.9396D − 03	3.9551D − 01	7.9322D − 01
	9.0141D − 01	7.6280D − 03	7.6280D − 03	9.1386D − 01	1.8353D + 00	−9.1385D − 01
4	9.3671D + 03	9.6784D − 01	1.1554D − 02	2.7664D − 02	7.7064D − 03	−8.4833D − 03
	−2.9877D − 01	−6.6809D − 02	6.6596D − 02	2.1916D − 02	−2.3099D − 02	−2.1655D − 02
5	9.3695D + 03	9.6796D − 01	−2.5295D − 02	2.3896D − 03	2.5379D − 02	−2.2747D − 03
	7.2457D − 01	−1.5034D − 04	−1.6038D − 04	−6.2335D − 02	−1.6662D − 04	−6.2291D − 02
6	9.3774D + 03	9.6837D − 01	2.0711D − 02	1.3384D − 03	2.3327D − 02	4.2746D − 02
	−4.0570D − 01	−2.1748D − 04	8.8020D − 06	−1.3474D + 00	8.4377D − 06	−1.3474D + 00
7	1.4434D + 04	1.2014D + 00	2.0228D − 02	3.3282D − 02	8.2397D − 03	−5.0500D − 03
	1.9964D − 02	−6.4706D − 02	7.6280D − 03	9.1386D − 01	1.8353D + 00	−9.1385D − 01
8	1.4438D + 04	1.2016D + 00	−2.7579D − 02	7.6191D − 03	2.7658D − 02	−7.1620D − 03
	−5.5421D − 02	8.5486D − 04	6.6596D − 02	2.1916D − 02	−2.3099D − 02	−2.1655D − 02
9	1.4449D + 04	1.2020D + 00	−2.1730D − 02	−3.5048D − 03	−3.0356D − 02	−4.8746D − 02
	−4.3834D − 02	−2.6446D − 03	−1.6038D − 04	−6.2335D − 02	−1.6662D − 04	−6.2291D − 02
10	2.9235D + 04	1.7098D + 00	3.5229D − 02	1.8941D − 02	−1.9101D − 02	−6.3917D − 03
	1.3349D − 02	−9.5809D − 02	−2.4859D − 04	4.9819D − 02	9.9311D − 02	−4.9942D − 02
11	2.9241D + 04	1.7100D + 00	1.2714D − 02	−3.2353D − 02	−1.8331D − 02	2.6496D − 02
	9.1395D − 02	−8.7025D − 04	8.8020D − 06	−1.3474D + 00	8.4377D − 06	−1.3474D + 00
12	2.9330D + 04	1.7126D + 00	−2.6764D − 02	−2.2095D − 02	−4.8248D − 02	−5.4552D − 02
	−7.6910D − 02	2.1980D − 02	7.6280D − 03	9.1386D − 01	1.8353D + 00	−9.1385D − 01
13	6.6137D + 04	2.5717D + 00	4.2064D − 03	−1.2611D − 02	−1.0889D − 02	5.1266D − 03
	−1.2750D + 00	−3.1969D − 04	6.6596D − 02	2.1916D − 02	−2.3099D − 02	−2.1655D − 02
14	6.6149D + 04	2.5719D + 00	−8.7250D − 03	−5.6175D − 03	−1.6050D − 02	−2.0932D − 02
	7.3611D − 01	5.2447D − 04	−1.6038D − 04	−6.2335D − 02	−1.6662D − 04	−6.2291D − 02
15	8.3393D + 04	2.8878D + 00	−1.0661D + 00	−1.0912D + 00	−1.9127D − 01	−1.6634D − 01
	5.4014D − 02	−1.0728D − 02	−2.4859D − 04	4.9819D − 02	9.9311D − 02	−4.9942D − 02
16	8.5845D + 04	2.9299D + 00	−1.2114D + 00	−1.2316D + 00	−1.6772D − 01	−1.4852D − 01
	8.6609D − 02	−5.7732D − 02	7.6280D − 03	9.1386D − 01	1.8353D + 00	−9.1385D − 01
17	1.0641D + 05	3.2620D + 00	1.6479D + 00	−1.6072D + 00	−8.5402D − 01	7.9900D − 01
	−6.7777D − 02	−3.6456D − 02	6.6596D − 02	2.1916D − 02	−2.3099D − 02	−2.1655D − 02
18	1.4505D + 05	3.8086D + 00	2.9756D − 01	3.4352D − 01	−2.2729D + 00	−2.3139D + 00
	−2.9456D − 02	1.0361D − 02	−1.6038D − 04	−6.2335D − 02	−1.6662D − 04	−6.2291D − 02
19	2.0536D + 05	4.5317D + 00	−1.2292D − 01	−6.9860D − 02	2.3551D − 01	1.9854D − 01
	−4.9391D − 02	−4.7065D − 03	−2.4859D − 04	4.9819D − 02	9.9311D − 02	−4.9942D − 02
20	2.2858D + 05	4.7810D + 00	7.4038D − 01	−7.6148D − 01	2.5116D + 00	−2.4833D + 00
	−2.1497D − 02	2.2803D − 02	−6.5015D − 02	2.2363D − 02	−1.8583D − 02	−2.3848D − 02

Table B1a The Kalman filter gain matrix G. Note that G only has three columns because one output channel (the last one) has been dropped in the design. See the text for the details

$$G = \begin{bmatrix}
-183.9546 & -113.1696 & 22.4899 \\
-78.8768 & -171.5629 & -46.0620 \\
-41.6075 & -7.6386 & 4.3053 \\
0.0815 & 38.5255 & 102.4117 \\
3.1034 & -4.7030 & 140.8968 \\
-27.1305 & 12.1648 & 29.5587 \\
-35.7649 & 64.6860 & 20.6612 \\
25.1675 & -5.7130 & -8.1067 \\
12.6495 & -3.2761 & -22.6667 \\
26.1888 & 8.7922 & 17.6726 \\
-5.0242 & -8.5171 & -18.0876 \\
-11.0940 & -4.5687 & 13.4912 \\
4.0329 & -7.3458 & -3.6531 \\
-37.1429 & 35.3148 & 4.8433 \\
-40.8833 & -27.9416 & 22.6078 \\
-5.4819 & 13.7862 & -11.8439 \\
-33.7461 & 22.1656 & -26.7362 \\
-14.6262 & 9.0838 & 1.4405 \\
9.3845 & -30.7222 & -27.4402 \\
2.4587 & -0.5667 & 0.9105 \\
1.1803 & -2.0013 & -0.2963 \\
-2.5736 & -0.7643 & -2.0165 \\
0.0981 & -1.0360 & -1.1727 \\
-1.4190 & -0.7889 & 0.6328 \\
-0.4595 & 0.9764 & -0.8228 \\
-2.4890 & -3.1714 & -2.5552 \\
-2.2556 & -4.1851 & -1.3418 \\
-0.6707 & 2.0444 & 1.1271 \\
-3.6732 & 1.0172 & -1.1443 \\
0.3047 & 0.9068 & 4.2929 \\
0.9087 & 1.4235 & 0.0438 \\
-0.0527 & -1.7044 & 0.6853 \\
-0.3576 & 0.2374 & 1.3281 \\
0.1341 & 1.4295 & -0.5032 \\
0.1375 & 0.0074 & -0.3505 \\
-0.1810 & -0.4877 & 0.5969 \\
0.5282 & 0.3937 & 0.7748 \\
-2.4817 & 0.6985 & 0.7895 \\
0.0836 & 0.7134 & -0.7542 \\
-0.1950 & 0.1117 & -0.5622 \\
0.3657 & 2.0337 & -0.3493 \\
-0.1440 & -0.1715 & -0.6369 \\
-0.3383 & 0.3449 & 0.3496 \\
-0.4932 & -0.1132 & -1.3466 \\
0.3293 & 0.1159 & 0.0508 \\
0.2996 & 0.2242 & 0.1587 \\
0.0172 & -0.0101 & 0.0065 \\
-0.0012 & -0.0113 & -0.0145
\end{bmatrix}$$

Table B1b The transpose of the state feedback gain matrix H^T of the linear quadratic controller

$$H^T = \begin{bmatrix}
-124.1559 & -171.9583 & -20.7225 & 27.9936 \\
-127.2029 & 52.3483 & 98.7551 & -80.8847 \\
-35.8471 & -22.3277 & 17.7765 & 6.4051 \\
15.3550 & 1.7371 & 68.3735 & 82.4884 \\
41.1056 & -22.2281 & 52.8319 & 115.9376 \\
-1.5253 & 7.6869 & 8.0425 & -1.9116 \\
45.1327 & 23.1955 & -1.5012 & 20.0718 \\
-13.0491 & -15.0457 & -0.5502 & 1.0950 \\
-16.6456 & -7.0161 & -28.1768 & -38.5337 \\
3.7120 & 0.5616 & -2.3931 & 0.7033 \\
-10.6281 & -5.7205 & -13.4824 & -18.2356 \\
12.9708 & 2.8316 & -1.0964 & 8.4918 \\
-29.8676 & -38.6228 & -4.9102 & 3.4927 \\
20.1945 & 18.5220 & 0.9693 & 2.4423 \\
19.0101 & -30.5320 & -48.5485 & 0.9374 \\
-6.7179 & -16.2703 & 10.0342 & 19.1849 \\
-20.3036 & -31.2063 & 12.0575 & 22.0397 \\
-13.5706 & -13.3657 & -2.8444 & -3.2476 \\
30.7913 & 4.0483 & 5.0020 & 31.9106 \\
-0.2363 & -2.3488 & -1.8698 & 0.2436 \\
1.5950 & 0.6638 & -0.7891 & 0.2272 \\
-0.2911 & -0.2414 & 1.0200 & 0.9948 \\
1.0673 & 1.3419 & -0.4765 & -0.8173 \\
0.6293 & -0.8317 & -1.3338 & 0.1140 \\
0.0706 & -0.5795 & -0.2671 & 0.3796 \\
-1.2192 & -0.1052 & 0.6362 & 0.5160 \\
0.7895 & -0.9377 & 0.3563 & 2.1553 \\
-0.0790 & -2.2109 & 0.1870 & 2.3684 \\
-0.5826 & 1.6589 & -0.3700 & -2.6666 \\
3.2034 & -1.7851 & 1.0252 & 6.1400 \\
-1.7712 & -1.5368 & 1.1154 & 1.2639 \\
1.2264 & 2.3192 & -0.9587 & -2.5633 \\
0.6087 & -0.2672 & -0.3502 & 0.6124 \\
-1.4740 & -1.3003 & 1.1244 & 1.4722 \\
0.3672 & 0.1962 & -0.2015 & -0.0263 \\
1.2453 & 0.8617 & -0.4935 & -0.4431 \\
-0.0305 & -0.0916 & -0.6416 & 0.0391 \\
-1.1438 & -1.7567 & -1.3293 & -0.4383 \\
-0.4647 & 0.1370 & 0.3961 & -0.2035 \\
0.3036 & 0.1001 & -0.3002 & -0.1556 \\
-1.1670 & 0.3744 & 1.2753 & -0.0967 \\
-0.1757 & -0.0901 & 0.0079 & -0.0453 \\
-0.0348 & 0.0807 & 0.0864 & 0.0050 \\
0.3944 & 0.0639 & 0.0919 & 0.3394 \\
0.0048 & -0.1097 & -0.1073 & 0.0078 \\
-0.1254 & 0.0695 & 0.0988 & -0.0904 \\
0.0117 & 0.0170 & 0.0006 & -0.0037 \\
0.0117 & -0.0051 & -0.0032 & 0.0128
\end{bmatrix}$$

where $c_i \in \mathbf{R}^{4\times 1}$, $b_i \in \mathbf{R}^{1\times 4}$, and $b_{mi} \in \mathbf{R}^{1\times 2}$ for all i. The data are provided in the following format

i	w_i^2 ζ_i	b_i
	b_{mi}	c_i^T

and appear in Table A1.

Appendix B

The structure of the full-order linear quadratic controller is delineated and the data of the controller are tabulated in this appendix. The linear quadratic controller along with the augmented plant can be visualized through the following diagram.

The matrices A_a, B_{oa}, B_{ma}, C_{ma}, and C_{oa} are defined as in Eqs. (12). The state feedback gain matrix is $G = K_f$; $H = (1/r_o)B_{oa}^T P_a$ is the Kalman filter gain matrix, as defined in the text. The full-order linear quadratic controller, gain matrices, are tabulated in Tables B1a and B1b.

Appendix C

The reduced-order controller $K_r(s)$ is of McMillan degree 10, i.e.,

$$K_r(s) = H_r(sI - F_r)^{-1}G_r$$

where $F_r \in \mathbf{R}^{10\times 10}$, $G_r \in \mathbf{R}^{10\times 3}$, and $H_r \in \mathbf{R}^{4\times 10}$. The data appear in Table C1.

Table C1 The reduced-order controller

F_r(first 5 cols.) =

−0.2812	−111.5147	−9.4406	9.7403	1.6410
112.8366	−4.5391	−28.4620	0.9214	−20.2403
9.5832	24.9240	−2.3732	86.0086	−11.0139
−10.4227	5.5836	−84.6255	−3.2637	40.1314
−2.5093	21.5587	11.0724	−40.1163	−1.4654
−8.5882	16.9790	−10.3136	−13.8360	−61.3014
−4.7233	8.2345	−12.8261	−7.3280	−28.7487
−2.2104	6.6124	5.0277	−1.3010	−6.3532
7.4640	−4.9263	−4.7248	0.4584	16.1355
0.7116	−6.1917	−9.4331	−0.7073	4.7113

F_r(last 5 cols.) =

5.4430	3.7112	2.3439	−7.5224	2.5246
4.6784	5.7999	−5.1642	−5.9608	−12.6826
12.5553	15.0769	−2.8163	−11.3967	−5.6689
−9.8325	−7.7392	−0.3783	9.5444	3.9272
61.5292	29.4800	6.1572	−15.4082	1.5797
−47.7384	−15.1563	−0.0937	−9.4071	−2.0750
−40.4868	−18.6328	−10.9476	66.9187	8.0620
−6.8350	6.8024	−2.8212	2.8317	−68.4756
40.8754	−45.7473	11.0687	−57.5540	−16.0567
0.0956	−4.4747	69.3403	4.7431	−62.1477

$G_r =$

−8.2558	−4.2382	−0.3464
22.9031	−19.3414	−22.4017
5.3726	−26.2993	−7.3008
−4.1681	12.4768	30.2890
−7.2146	−3.7854	−21.7344
−13.2090	3.9421	148.9836
0.5975	39.1257	88.1060
37.3584	4.2523	14.1363
−72.8968	−176.1904	−45.0719
188.6996	−111.0931	24.9621

$H_r^T =$

6.3838	0.5933	0.8063	6.6698
−20.4253	−13.2346	−16.1584	−23.3887
−21.6990	−11.8567	12.3534	3.1281
8.8379	−0.7220	17.4077	26.6235
14.3909	4.6409	6.1431	16.5043
46.2858	−16.6639	63.3823	126.2883
11.1762	0.8607	61.9255	73.0303
33.2331	21.1439	−2.4465	7.4887
−138.3783	45.9850	100.3133	−84.0389
−122.1205	−178.6393	−21.7788	35.6737

Acknowledgments

This paper was supported in part by JSEP Grant F49620-88-C-0067 and in part by Air Force Office of Scientific Research Grant 85-0256.

The authors wish to thank R. Benhabib and C. Major of TRW for providing them with the data of the TRW experimental structure.

References

[1]Moore, B. C., "Principal Component Analysis in Linear Systems: Controllability, Observability and Model Reduction," *IEEE Transactions on Automatic Control*, Vol. AC-26, Jan. 1981, pp. 17–32.

[2]Glover, K., "All Optimal Hankel-Norm Approximations of Linear Multivariable Systems and Their Error Bounds," *International Journal of Control*, Vol. 39, June 1984, pp. 1115–1193.

[3]Opdenacker Ph. and Jonckheere, E. A., "A Contraction Mapping Preserving Balanced Reduction Scheme and Its Infinity Norm Error Bounds," *IEEE Transactions on Circuits and Systems*, Vol. CAS-35, Feb. 1988, pp. 141–149.

[4]Jonckheere, E. A. and Silverman, L. M., "Singular Value Analysis of Deformable Systems," *Circuits, Systems and Signal Processing*, Vol. 1, No. 3-4, 1982, pp. 447–470.

[5]Jonckheere, E. A. and Opdenacker, Ph., "Singular Value Analysis, Balancing and Model Reduction of Large Space Structures," *Proceedings of American Control Conference* (ACC-84), Session WA6-3, Inst. of Electrical and Electronics Engineers, Piscataway, NJ, 1984.

[6]Pernebo, L. and Silverman, L. M., "Model Reduction Via Balanced State Space Representation," *IEEE Transactions on Automatic Control*, Vol. AC-27, April 1982, pp. 382–387.

[7]Opdenacker, Ph. and Jonckheere, E. A., "LQG Balancing and Reduced LQG Compensation of Symmetric Passive Systems," *International Journal of Control*, Vol. 41, Jan. 1985, pp. 73–109.

[8]Enns, D., "Model Reduction with Balanced Realizations: An Error Bound and a Frequency Weighted Generalization," *Proceedings of IEEE Conference on Decision and Control*, Inst. of Electrical and Electronics Engineers, Piscataway, NJ, 1984.

[9]Kallstrom, C., "Computing EXP(A) and $\int$ EXP(As)ds," Rept. 7309, Lund Inst. of Technology, Div. of Automatic Control, March 1973.

[10]Jonckheere, E. A., "Principal Component Analysis of Flexible Systems—Open-Loop Case," *IEEE Transactions on Automatic Control*, Vol. AC-29, Dec. 1984, pp. 1095–1097.

[11]Safonov, M. G., Laub, A. J., and Hartmann, G. L., "Feedback Properties of Multivariable Systems: The Role and Use of the Return Difference Matrix," *IEEE Transactions on Automatic Control*, Vol. AC-26, Feb. 1981, pp. 47–65.

[12]Jonckheere, E. A., "A Closed-Loop Principal Component Analysis of a Tetrahedral Truss," *Proceedings Workshop on Applications of Distributed System Theory to the Control of Large Space Structures*, Jet Propulsion Lab., California Inst. of Technology, Pasadena, CA, NASA-Jet Propulsion Lab. Pub. 83-46, 1983, pp. 163–180.

[13]Doyle, J. C. and Stein, G., "Multivariable Feedback Design: Concepts for a Classical/Modern Synthesis," *IEEE Transactions on Automatic Control*, Vol. AC-26, No. 1, Feb. 1981, pp. 4–16.

[14]Laub, A. J., "A Schur Method for Solving Algebraic Riccati Equations," *IEEE Transactions on Automatic Control*, Vol. AC-24, Dec. 1979, pp. 913–921.

[15]Safonov, M. G. and Athans, M., "Gain and Phase Margin for Multiloop LQG Regulators," *IEEE Transactions on Automatic Control*, Vol. AC-22, No. 2, April, 1977, pp. 173–178.

[16]Doyle, J. C., "Guaranteed Margins for LQG Regulators," *IEEE Transactions on Automatic Control*, Vol. AC-23, No. 4, Aug. 1978, p. 756.

[17]Laub, A. J., "On Computing Balancing Transformations," *Proceedings of 1980 Joint American Control Conference*, Session FA8-E, Inst. of Electrical and Electronics Engineers, Piscataway, NJ, 1980.

[18]Opdenacker, Ph. C., "Balanced Model Order Reduction Techniques and Their Applications to Large Space Structure Problems," Ph.D. Dissertation, Dept. of Electrical Engineering-Systems, Univ. of Southern California, Los Angeles, CA, 1985.

[19]Kwakernaak, H. and Sivan, R., *Linear Optimal Control Systems*, Wiley-Interscience, New York, 1972.

[20]Major, C. S. and Simonian, S. S., "An Experiment to Demonstrate Active and Passive Control of a Flexible Structure. *Proceedings of American Control Conference*, Session TA-6, Inst. of Electrical and Electronics Engineers, Piscataway, NJ, June 1984.

[21]Juang, J. C. "H^w Control: Its Structure and Computation" Ph.D. Thesis, Dept. of Electrical Engineering, Univ. of Southern California, Los Angeles, CA, 1987

[22]Lukich, M. S., and Tung, F. C., "Experimental Verification of Control and System Identification Techniques for a Flexible Truss Structure," *Proceedings of 1986 American Control Conference*, Inst. of Electrical and Electronics Engineers, Piscataway, NJ, 1986.